

**Magnetic structure of CoO studied by neutron and synchrotron x-ray diffraction**K. Tomiyasu,<sup>1,\*</sup> T. Inami,<sup>2</sup> and N. Ikeda<sup>3</sup><sup>1</sup>*Department of Applied Physics, School of Science and Engineering, Waseda University,  
3-4-1 Ohkubo, Shinjuku, Tokyo 169-8555, Japan*<sup>2</sup>*Synchrotron Radiation Research Center, Japan Atomic Energy Research Institute, Mikazuki-cho, Hyogo 679-5148, Japan*<sup>3</sup>*Japan Synchrotron Radiation Research Institute, Hyogo 679-5198, Japan*

(Received 12 March 2004; revised manuscript received 21 June 2004; published 9 November 2004)

Below  $T_N=289$  K, the antiferromagnet CoO exhibits magnetic long-range order described by a propagation vector along the trigonal axis, whereas the lattice is distorted monoclinically along both the tetragonal and the trigonal axes. In order to elucidate this inconsistency, we performed neutron and synchrotron x-ray diffraction experiments on single crystals of CoO, and found a series of magnetic reflections represented by a propagation vector along the tetragonal axis below  $T_N$ . These results suggest an altered magnetic structure of CoO, which includes both the trigonal and the tetragonal propagation vectors, has a monoclinic symmetry, and which is in accordance with the distorted lattice symmetry.

DOI: 10.1103/PhysRevB.70.184411

PACS number(s): 75.25.+z

**I. INTRODUCTION**

The 3d transition metal monoxides MnO, FeO, CoO, and NiO have the cubic NaCl crystal structure in their paramagnetic phases, and the magnetic ions compose the fcc lattice. Below  $T_N$ , all these oxides exhibit the type-II-fcc antiferromagnetic (AF-II) order with a propagation vector  $\mathbf{Q}_{II} = (\frac{1}{2}, \frac{1}{2}, \frac{1}{2})$ .<sup>2</sup> In the AF-II order, ferromagnetic sheets of (111) planes are antiferromagnetically stacked along the [111] direction, as shown in Fig. 1(a). A crystallographic distortion occurs at the temperature  $T_N$  of antiferromagnetic ordering. Below  $T_N$ , the lattices of MnO, FeO, and NiO are distorted trigonally along the [111] direction and thus the symmetry of the lattice is consistent with that of the magnetic structure.<sup>3-5</sup> In contrast, CoO exhibits a tetragonal lattice distortion along the [001] direction below  $T_N$  and thus the lattice distortion and the magnetic propagation vector contradict each other in CoO.<sup>6,7</sup>

This inconsistency in CoO properties has attracted much interest both theoretically and experimentally for more than 40 years. For example, one can mention the debate on the AF-II structure versus Roth and van Laar's multi-spin-axis magnetic structure. The multi-spin-axis magnetic structure is consistent with the tetragonal lattice distortion and keeps the same  $\mathbf{Q}_{II}$ .<sup>1,8</sup> In addition, it gives the same neutron powder diffraction pattern as that of the AF-II structure.<sup>1,8</sup> Hartree-Fock calculations showed that CoO can take either the AF-II structure or the multi-spin-axis magnetic structure.<sup>9</sup> However, Herrmann-Ronzaud *et al.* carried out neutron diffraction experiments on single crystals under uniaxial stress applied along various directions and concluded that the magnetic structure of CoO is unambiguously the AF-II structure.<sup>10</sup>

Recently, a high resolution x-ray diffraction study of a powder specimen unambiguously revealed a small but finite trigonal lattice distortion accompanying the main tetragonal one,<sup>11</sup> which was previously suggested by x-ray diffraction experiments on a single crystal.<sup>12</sup> Jauch *et al.* deduced that the combination of the two components of the lattice distortion

changes the crystal symmetry below  $T_N$  from tetragonal into monoclinic.<sup>11</sup> Furthermore, they pointed out that the odd direction of the magnetic moments, which was determined as the  $[0.325\ 0.325\ 0.888]$  direction by neutron powder diffraction,<sup>1</sup> is in the monoclinic  $a'b'$  plane.<sup>11</sup> Thus, we suspected the magnetic structure of CoO to exhibit a more explicit monoclinic symmetry including not only the trigonal  $\mathbf{Q}_{II}$ , but also another tetragonal propagation vector. The present article reports our reinvestigation of the magnetic order using neutron and synchrotron x-ray diffraction experiments on single crystals of CoO.

In neutron diffraction experiments, new reflections represented by the propagation vector  $\mathbf{Q}_I = (0, 0, 1)$  (along the tetragonal axis) were found below  $T_N$ . Subsequent synchrotron x-ray diffraction experiments confirmed that these reflections have a magnetic origin. Therefore, the type-I-fcc antiferromagnetic (AF-I) order, in which ferromagnetic (001) planes are alternately stacked along the tetragonal [001] axis [Fig. 1(b)], coexists with the conventional AF-II order below  $T_N$ . The direction of the AF-I component of magnetic moments is determined from neutron data and finally a monoclinic magnetic structure of CoO is proposed, obtained by superposing the AF-I component on the AF-II component.

**II. EXPERIMENTS**

Neutron diffraction experiments were performed on the T1-1 triple axis spectrometer installed at a thermal guide of JRR-3M, Tokai, Japan. The energy of the incident neutrons was fixed at 13.5 meV. Pyrolytic graphite filters eliminated the half-lambda contamination down to the order of  $10^{-6}$ . Synchrotron x-ray diffraction experiments were performed using a four-circle diffractometer installed at the beamline BL02B1, SPring-8, Japan. The energy of the incident photons was fixed at 7.66 keV below the Co *K*-edge absorption edge.<sup>13</sup> In both diffraction experiments, samples were mounted on the cold finger of closed-cycle He refrigerators.

Single-crystal A with a size of about  $15 \times 8 \times 2$  mm<sup>3</sup> was used for the neutron diffraction experiments. Single-crystal B

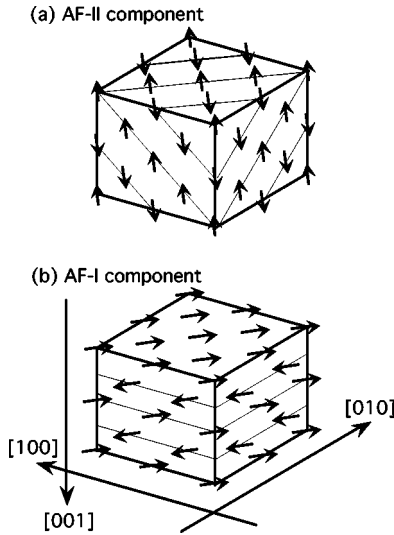


FIG. 1. AF-II order (a) and AF-I order (b). In (a), the magnetic moments tilt along the  $[0.325\ 0.325\ 0.888]$  direction, as reported by van Laar (Ref. 1). In (b), the direction of the magnetic moments is parallel to the  $[1\bar{1}0]$  direction.

with a size of about  $5 \times 1 \times 1\text{ mm}^3$  was used for the synchrotron x-ray diffraction experiments. Parts of the crystals were ground to powder form for chemical analysis and x-ray powder diffraction experiments. By chemical analysis, the molar ratio of Co:Ni:Fe:O was shown to be 0.996:0.003:0.001:1. In an x-ray powder diffraction pattern at room temperature, no extra lines, which could not be explained by the NaCl structure, were observed. The crystal mosaic was estimated to be about  $10'$  at 50 K.

### III. RESULTS AND DISCUSSION

#### A. Neutron diffraction

The magnetic reflections due to the AF-II order appear at the  $h/2\ k/2\ l/2$  reciprocal lattice points, where  $h, k,$  and  $l$  are all odd.<sup>2</sup> In addition to these conventional magnetic reflections, we found additional reflections at 001, 110, 112, and 221 in our neutron diffraction experiments. As shown in

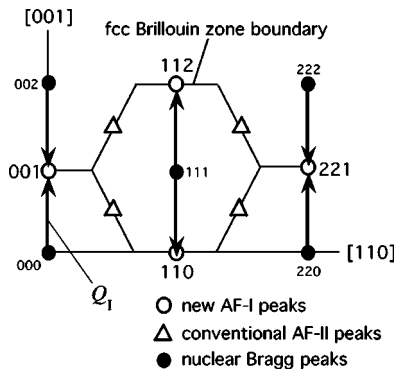


FIG. 2. Schematic map of three kinds of the reflections on the  $(hhl)$  zone. The arrows indicate the propagation vector  $Q_1 = (0, 0, \pm 1)$ .

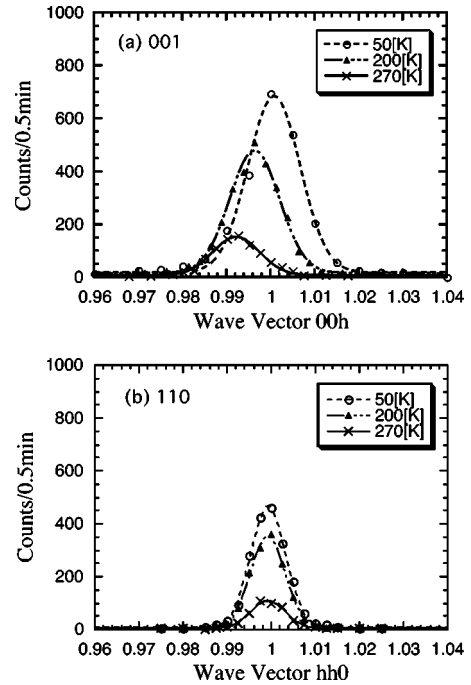


FIG. 3. Neutron diffraction line profiles of the 001 reflection (a) and the 110 reflection (b) below  $T_N=289\text{ K}$ . Data (a) and data (b) were taken by scanning along the  $[001]$  direction and the  $[110]$  direction, respectively. As the temperature increases, the 001 reflection shifts towards the origin 000 because of the tetragonal lattice contraction.

Fig. 2, all these reflections are described by propagation vector  $Q_1$ .

We show the temperature evolution of the line profiles of the 001 and 110 reflections and the integrated intensity of the 001 reflection in Figs. 3 and 4, respectively. The diffraction intensity decreases with increasing temperature, and finally disappears at  $T_N$ . The diffraction intensity of the  $Q_1$  reflections is an order parameter of the transition at  $T_N$  as well as that of the  $Q_{II}$  magnetic reflections. These reflections are ascribed to either the ordering of magnetic moments or the modulation of lattice distortion, which has not been reported so far.

Table I gives the integrated intensity of the  $Q_1$  reflections. As the magnitude of the scattering vector  $K=(h, k, l)$  in-

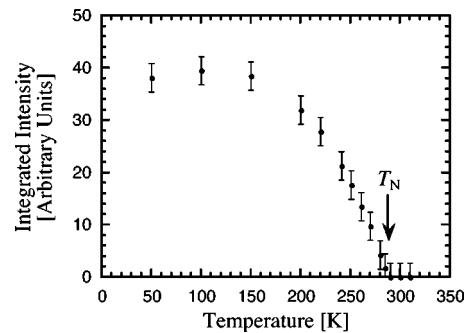


FIG. 4. Temperature dependence of the neutron diffraction intensity of the 001 reflection.

TABLE I. Experimental integrated intensity of the  $Q_1$  magnetic reflections on the  $(hkl)$  zone and best-fit calculated one. The experimental intensity was measured at 50 K. The best-fit calculated intensity was obtained when the AF-I component of magnetic moments lies within the tetragonal  $c$  plane (transverse wave).

$hkl$	Experimental	Calculated
001	1143	1040
110	785	891
112	317	263
221	262	243

creases, the intensity of the  $hkl$  reflection decreases. This fact indicates that the  $Q_1$  reflections depend on the magnetic form factor and come from magnetic scattering. Actually, the intensity will be explained by using the Watson-Freeman magnetic form factor of the  $\text{Co}^{2+}$  ion<sup>14</sup> in Sec. III C. In contrast, if the  $Q_1$  reflections arise from the nuclear scattering, the intensity does not decrease with increasing the magnitude of  $\mathbf{K}$ .

It also should be mentioned that the ordered state represented by the  $Q_1$  reflections is long-range order. The line widths of the  $Q_1$  reflections are as sharp as those of the nuclear Bragg reflections at 002, 220, and so on. The correlation length of the ordered state estimated from the line widths is longer than the instrumental resolution limit of 50 nm.

### B. Synchrotron x-ray diffraction

In order to obtain other evidence supporting that the  $Q_1$  reflections are due to the ordering of magnetic moments and not to the modulation of lattice distortion, we performed synchrotron x-ray diffraction experiments and compared the x-ray data with the neutron data. In x-ray diffraction, magnetic scattering is much weaker than the conventional Thomson scattering owing to the factor  $(\hbar\omega/mc^2)^2 \approx 10^{-4}$ , where  $\hbar\omega$  is the energy of the incident photons and  $mc^2$  is the rest energy of an electron, respectively. Therefore, if the  $Q_1$  reflections are magnetic scattering, the value of  $I(001)/I(002)$  from x-ray data must be much smaller than that from neutron data, where  $I(hkl)$  stands for the scattering intensity of the  $hkl$  reflection, because the 002 fundamental reflection arises from the Thomson scattering. On the other hand, the values of  $I(001)/I(\frac{3}{2}\frac{3}{2}\frac{3}{2})$  from both data must be of the same order, because the  $\frac{3}{2}\frac{3}{2}\frac{3}{2}$  reflection is also magnetic scattering. In contrast, if the  $Q_1$  reflections come from the modulation of lattice distortion, the values of  $I(001)/I(002)$  from both data should be of the same order, while the value of  $I(001)/I(\frac{3}{2}\frac{3}{2}\frac{3}{2})$  from x-ray data will be larger than that from neutron data.

Figure 5 shows scan data around the 001 and  $\frac{3}{2}\frac{3}{2}\frac{3}{2}$  reciprocal lattice points obtained at 50 K in our synchrotron x-ray diffraction experiments on a single crystal. The 001 reflection was not observed within statistical uncertainty. Table II gives the values of  $I(001)/I(\frac{3}{2}\frac{3}{2}\frac{3}{2})$  and  $I(001)/I(002)$ . As shown in Table II, the value of  $I(001)/I(002)$  from x-ray data is much smaller than that from neutron data, whereas the

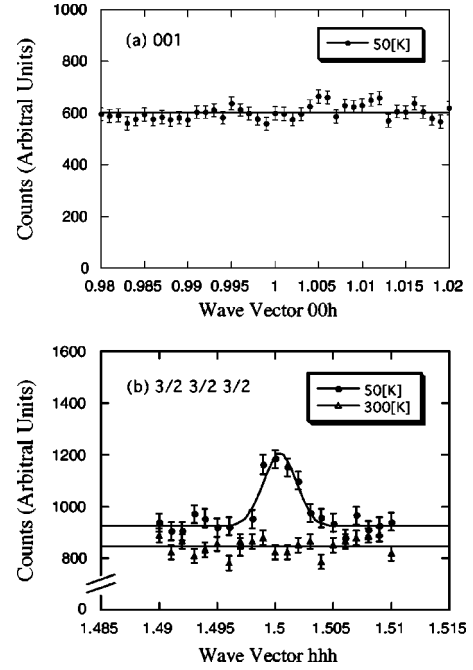


FIG. 5. Scan data around 001 (a) and  $\frac{3}{2}\frac{3}{2}\frac{3}{2}$  (b) in synchrotron x-ray diffraction experiments. Data (a) and data (b) were taken by scanning along the [001] direction and the [111] direction, respectively.

value of  $I(001)/I(\frac{3}{2}\frac{3}{2}\frac{3}{2})$  from x-ray data is, at most, not far larger than that from neutron data. Thus, we conclude that the 001 reflection unambiguously is due to magnetic scattering. The ordered state represented by  $Q_1$  is interpreted as the AF-I order of magnetic moments.

### C. AF-I component

In the present section, we show that the AF-I component of a magnetic moment  $\mathbf{M}_I$  points to the  $[1\bar{1}0]$  direction. The direction is obtained by combining the two following conditions,  $\mathbf{M}_I \perp [001]$  and  $\mathbf{M}_I \perp \mathbf{M}_{II}$ , where  $\mathbf{M}_{II}$  is the AF-II component of a magnetic moment. The  $\mathbf{M}_{II}$  vector is parallel to the  $[0.325\ 0.325\ 0.888]$  direction,<sup>1</sup> as mentioned in Sec. I.

The first condition,  $\mathbf{M}_I \perp [001]$ , was obtained from analyzing the experimental integrated intensity of the  $Q_1$  magnetic reflections, given in Table I. The intensity was calculated by varying the direction of  $\mathbf{M}_I$  so as to best fit the experimental values in a least-squares method. For the calculations, the following equation was used:

TABLE II. Ratio of the integrated intensity of the 001 reflection to those of the  $\frac{3}{2}\frac{3}{2}\frac{3}{2}$  and 002 reflections. The values from x-ray data are compared to those from neutron data.

Ratio	X-ray	Neutron
$I(001)/I(002)$	$\leq 10^{-8}$	$10^{-3}$
$I(001)/I(\frac{3}{2}\frac{3}{2}\frac{3}{2})$	$\leq 10^{-2}$	$10^{-3}$

$$I(\mathbf{K}) = C L(\mathbf{K}) |F(\mathbf{K})|^2 \sum_{j=1}^4 \frac{|\mathbf{K} \times (\mathbf{M}_j \times \mathbf{K})|^2}{|\mathbf{K}|^4}, \quad (1)$$

where  $I$  is a diffraction intensity,  $\mathbf{K}$  is a scattering vector,  $C$  is a constant value,  $L$  is the Lorentz factor  $1/\sin 2\theta$ ,  $F$  is the Watson-Freeman magnetic form factor of the  $\text{Co}^{2+}$  ion,<sup>14</sup>  $j$  is the multiplicity of the monoclinic domains, and  $\mathbf{M}_j$  is the magnetic moment of the  $\text{Co}^{2+}$  ion in the  $j$ th domain.

We took into account only four kinds of monoclinic domains coming from the four trigonal axes as the multiplicity of  $j$ . Since the lattice distortion of CoO is monoclinic and consists of a tetragonal component and a trigonal component, there are twelve types ( $=3 \times 4$ ) of monoclinic domains in CoO, characterized by the three tetragonal axes and the four trigonal axes. However, taking the  $(hhl)$  zone as the scattering plane in our neutron scattering experiments, we extracted only one tetragonal axis along the  $[001]$  direction, as shown in Fig. 2. Hence, the observed  $Q_1$  magnetic scattering includes only the contribution from the four types of monoclinic domains with one tetragonal axis and the four trigonal axes.

The secondary extinction effect of the  $Q_1$  magnetic reflections was ignored, because these reflections were as weak as of the order of  $10^{-3}$  times the  $\frac{111}{222}$  magnetic reflection. The exact ratio of the scattering intensity is further reduced by the secondary extinction effect of the strong  $\frac{111}{222}$  magnetic reflection. The weak intensity would explain why the  $Q_1$  magnetic reflections have not been found so far.

The second condition,  $\mathbf{M}_I \perp \mathbf{M}_{II}$ , is derived as follows. We can assume every  $\text{Co}^{2+}$  ion to possess a magnetic moment with the same magnitude, because hyperfine Mössbauer spectra of  $^{57}\text{Fe}$  in CoO can be analyzed by a single hyperfine magnetic field.<sup>15</sup> This assumption is also supported by a recent  $\gamma$ -ray diffraction study, in which highly accurate structure factors are described by a single-electron density of  $\text{Co}^{2+}$  ion.<sup>16</sup> Adding up the AF-I component and the AF-II component, one obtains

$$|\mathbf{M}_I + \mathbf{M}_{II}| = |\mathbf{M}_I - \mathbf{M}_{II}|, \quad (2)$$

therefore

$$\mathbf{M}_I \perp \mathbf{M}_{II}. \quad (3)$$

#### D. Magnetic structure

In Secs. III A–III C, it was shown that the AF-I component and the conventional AF-II component coexist below  $T_N$  in CoO. Each magnetic component is illustrated in Figs. 1(a) and 1(b). We propose a magnetic structure of CoO obtained by superposing the AF-I component on the AF-II component. Figures 6(a) and 6(b) show the magnetic structure and the monoclinic magnetic primitive unit cell, respectively.

We would like to mention that the present magnetic structure is consistent with the lattice distortion in terms of symmetry. First, the lattice distortion is composed of a tetragonal component and a trigonal component, and the present magnetic structure includes a tetragonal  $Q_1$  and a trigonal  $Q_{II}$  simultaneously. Second, the  $\mathbf{M}_I$  vector is parallel to the  $c'$

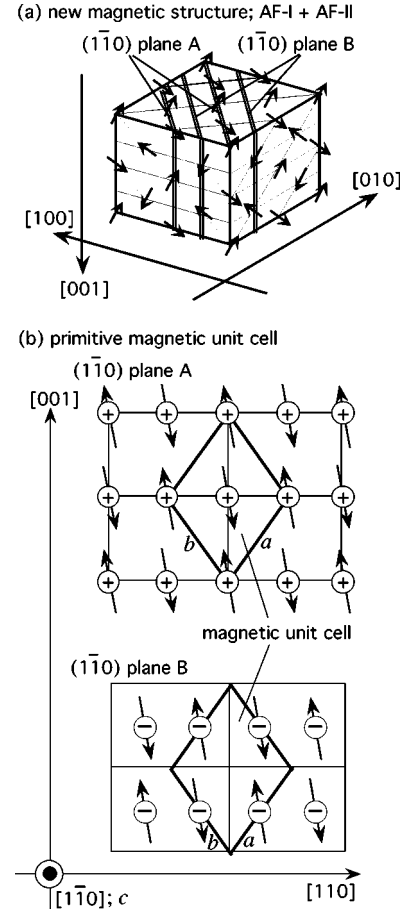


FIG. 6. (a) Magnetic structure of CoO. The AF-I component is exaggerated. (b) Monoclinic primitive unit cell of the magnetic structure, projected on the  $(1\bar{1}0)$  A plane and the  $(1\bar{1}0)$  B plane. The relation between the face-centered unit cell and these A and B planes is shown in (a). The symbols + and - identify the collinear AF-I component of magnetic moments along the  $c'$  axis with respect to the magnetic unit cell. The arrows represent the collinear AF-II component of magnetic moments within the  $a'b'$  plane with respect to the magnetic unit cell.

axis with respect to the monoclinic magnetic unit cell (the  $[1\bar{1}0]$  direction), and the  $\mathbf{M}_{II}$  vector lies in the  $a'b'$  plane with respect to the monoclinic magnetic unit cell, as shown in Fig. 6(b).

The diffraction intensity of the  $Q_1$  magnetic reflections was much weaker than that of the  $Q_{II}$  magnetic reflections in our neutron experiments. From the ratio of diffraction intensities, the magnitude of  $\mathbf{M}_I$  is estimated to be less than 5% of that of  $\mathbf{M}_{II}$ . Nevertheless, the magnitude of the tetragonal component of the lattice distortion is far larger than that of the trigonal one. This apparent incompatibility is not a surprise. The combination of  $(J_1, J_2)$ , where  $J_1$  is the nearest-neighbor  $90^\circ$  exchange integral and  $J_2$  is the second neighbor  $180^\circ$  exchange integral, was estimated as  $(-6.9 \text{ K}, -21.6 \text{ K})$ ,  $(-1.0 \text{ K}, -16.6 \text{ K})$ ,  $(-3.0 \text{ K}, -17.6 \text{ K})$ ,  $(-2.4 \text{ K}, -16.6 \text{ K})$ , and so on by many investigators,<sup>17–19</sup> as well, both  $J_1$  and  $J_2$  are antiferromagnetic and  $|J_2|$  is much more dominant than  $|J_1|$ . The second-neighbor correlation in the AF-II



component is antiferromagnetic, in compliance with the large antiferromagnetic  $J_2$  [Fig. 1(a)], while that in the AF-I component is ferromagnetic against  $J_2$  [Fig. 1(b)]. Therefore, the AF-I component should be much smaller than the AF-II component.

The quantitative treatment is complex, because the coexistence of the magnetic propagation vectors of different symmetry needs higher order kinematic exchange interactions, such as the biquadratic exchange interaction and the four-body exchange interaction, besides the Heisenberg Hamiltonian. This fact would suggest the importance of electron hopping and electron correlation for the magnetic order in CoO, which is consistent with Jauch *et al.*'s reports.<sup>16</sup> The unusual magnetic structure was actually explained by these interactions in NiS<sub>2</sub>.<sup>20,21</sup> NiS<sub>2</sub> is also a system in which magnetic ions form the fcc lattice and the magnetic order consists of both the AF-I and the AF-II components below  $T_N = 31$  K.<sup>22,23</sup> A detailed theory of CoO including such higher order exchange interactions is needed.

There have been discussions on whether the lattice distortion is due to the Jahn-Teller effect (structural) or to magnetostriction (magnetic). Kugel *et al.* explained it as the Jahn-Teller effect coming from the anisotropic electron clouds of Co<sup>2+</sup> ions ( $d^7$ ).<sup>24</sup> In contrast, Jauch *et al.* considered that magnetostriction is rather plausible because the symmetry reduction from cubic into monoclinic and the magnetic order occur at the same temperature  $T_N$ , which is contrary to what they expected if lattice distortion is due to the Jahn-Teller effect.<sup>11</sup> However, Reichtin *et al.* showed the strong magnetic short-range correlation with  $Q_{II}$  to persist even at 310 K (quite above  $T_N = 289$  K) by neutron diffraction,<sup>19</sup> suggesting that magnetic long-range order cannot be maintained without lattice distortion. Thus, neither the Jahn-Teller effect nor magnetostriction provides a satisfactory explanation for the lattice distortion.

To elucidate the origin of the lattice distortion, we make the following assumption. The strong magnetic short-range correlation in the paramagnetic phase arises from magnetic geometrical frustration. The monoclinic lattice distortion suppresses the magnetic geometrical frustration and brings about the magnetic order below  $T_N$ .

In the paramagnetic phase, the magnetic Co<sup>2+</sup> ions compose the fcc lattice. The fcc lattice is constructed by four simple-cubic (sc) sublattices, and the nearest-neighbor ions form tetrahedrons among the sc sublattices, as shown in Fig. 7. Giving the large antiferromagnetic  $J_2$  domination, we first arrange the magnetic moments on each sc sublattice in an Ising configuration, as also shown in Fig. 7. The arrangement includes no frustration. However, the correlation between the nearest-neighbor ions on the sc sublattices is frustrated because of the special atomic configuration of the tetrahedron and the antiferromagnetic  $J_1$ . Therefore, the magnetic correlation dynamically changes among the inter-sc-sublattices retaining the basic arrangements in the intra-sc-sublattices in the paramagnetic phase. Reichtin *et al.*'s strong magnetic short-range correlation must be caused by this frustration. It also would be worth noting that this frustration is identical to a degeneracy between the AF-II order and the multi-spin-axis magnetic structures, which is consistent with the Hartree-Fock calculations in the cubic phase.<sup>9</sup>

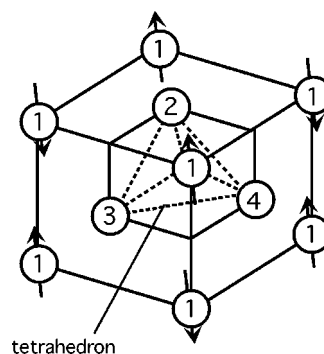


FIG. 7. The fcc lattice resolved into the four sc sublattices 1, 2, 3, and 4. The arrows are arranged so as to become antiferromagnetic between two 180° second-neighbor ions.

Such a frustration, which is caused by the tetrahedrons in the fcc lattice, was actually confirmed in a similar system, NiS<sub>2</sub>, by recent neutron scattering experiments.<sup>25</sup> Therefore, it is plausible that it exists in CoO as well. However, the frustration of NiS<sub>2</sub> differs from that of CoO because  $|J_1|$  is larger than  $|J_2|$  in NiS<sub>2</sub>.<sup>25</sup> There are no basic antiferromagnetic arrangements in the intra-sc-sublattices with  $Q_{II}$ , and the frustrated spin correlation is represented by many propagation vectors along the fcc Brillouin zone boundary in NiS<sub>2</sub>.<sup>25</sup>

At the temperature  $T_N$ , the lattice in CoO is distorted trigonally in order to suppress the frustration and this transforms the short-range order into the long-range AF-II order. However, the trigonal lattice distortion does not affect the equilateral triangular lattices on the (111) planes, which can cause frustration. Therefore, the tetragonal lattice distortion further occurs and leads to the long-range AF-I order. The existence of anisotropic electron clouds would further help the tetragonal lattice distortion in particular. This is supported by the pseudotetragonal shape of the electron clouds, which was recently obtained below  $T_N$  in the  $\gamma$ -ray diffraction study.<sup>16</sup> Thus, the concept of magnetic geometrical frustration provides a qualitatively reasonable interpretation of both the monoclinic lattice distortion and the present monoclinic magnetic order.

#### IV. CONCLUSIONS

We performed neutron and synchrotron x-ray diffraction experiments on single crystals of CoO. It was found that the additional  $Q_I$  magnetic reflections coexist with the well-known  $Q_{II}$  magnetic reflections below  $T_N$ . This fact indicates that the magnetically ordered state of CoO includes the AF-I component in addition to the AF-II component. We proposed a magnetic structure obtained by superposing the AF-I component on the AF-II component. The resulting magnetic structure has a monoclinic unit cell, in accordance with the distorted lattice symmetry.

The present complex magnetic structure needs other magnetic interactions, such as biquadratic exchange interaction

and four-body exchange interaction, besides the Heisenberg Hamiltonian. The concept of magnetic geometrical frustration can qualitatively explain both the monoclinic lattice distortion and the monoclinic magnetic order. Further theoretical and experimental investigation, taking into account these higher order exchange interactions and the magnetic geometrical frustration, are required to clarify the mechanism of magnetic order of CoO.

#### ACKNOWLEDGMENTS

We thank Prof. H. Kondoh for giving us the single crystals of CoO. We also thank Prof. Y. Tsunoda and Dr. H. Ohsumi for reading the present paper and giving us their fruitful advice. Our synchrotron x-ray diffraction experiments were performed at the SPring-8 facility with the approval of the Japan Synchrotron Radiation Research Institute (JASRI) (Proposal No. 2003A0580-ND1-np).

\*E-mail: k-tommy@aoni.waseda.jp

- <sup>1</sup>B. van Laar, Phys. Rev. **138**, A584 (1965).  
<sup>2</sup>C. G. Shull, W. A. Strauser, and O. Wollan, Phys. Rev. **83**, 333 (1951).  
<sup>3</sup>B. Morosin, Phys. Rev. B **1**, 236 (1970).  
<sup>4</sup>B. T. M. Willis and H. P. Rooksby, Acta Crystallogr. **6**, 827 (1953).  
<sup>5</sup>L. C. Bartel and B. Morosin, Phys. Rev. B **3**, 1039 (1971).  
<sup>6</sup>N. C. Tombs and H. P. Rooksby, Nature (London) **3165**, 442 (1950).  
<sup>7</sup>K. H. Germann, K. Maier, and E. Strauss, Phys. Status Solidi B **61**, 449 (1974).  
<sup>8</sup>W. L. Roth, Phys. Rev. **111**, 772 (1958).  
<sup>9</sup>T. Shishidou and T. Jo, J. Phys. Soc. Jpn. **67**, 2637 (1998).  
<sup>10</sup>D. Herrmann-Ronzaud, P. Burlet, and J. Rossat-Mignod, J. Phys. C **11**, 2123 (1978).  
<sup>11</sup>W. Jauch, M. Reehuis, H. J. Bleif, F. Kubanek, and P. Pattison, Phys. Rev. B **64**, 052102 (2001).  
<sup>12</sup>S. Saito, K. Nakahigashi, and Y. Shimomura, J. Phys. Soc. Jpn. **21**, 850 (1966).  
<sup>13</sup>W. Neubeck and C. Vettier, Phys. Rev. B **60**, R9912 (1999).  
<sup>14</sup>R. E. Watson and A. J. Freeman, Phys. Rev. **120**, 1134 (1960).  
<sup>15</sup>H. N. Ok and J. G. Mullen, Phys. Rev. **168**, 563 (1968).  
<sup>16</sup>W. Jauch and M. Reehuis, Phys. Rev. B **65**, 125111 (2002).  
<sup>17</sup>J. S. Smart, *Effective Field Theories of Magnetism* (W. B. Saunders, Philadelphia, 1966).  
<sup>18</sup>J. Sakurai, W. J. L. Buyers, R. A. Cowley, and G. Dolling, Phys. Rev. **167**, 510 (1968).  
<sup>19</sup>M. D. Reichtin and B. L. Averbach, Phys. Rev. B **5**, 2693 (1972).  
<sup>20</sup>A. Yoshimori and H. Fukuda, J. Phys. Soc. Jpn. **46**, 1663 (1979).  
<sup>21</sup>K. Yosida and S. Inagaki, J. Phys. Soc. Jpn. **50**, 3268 (1981).  
<sup>22</sup>J. M. Hasting and L. M. Corliss, IBM J. Res. Dev. **14**, 227 (1970).  
<sup>23</sup>K. Kikuchi *et al.*, J. Phys. Soc. Jpn. **45**, 444 (1978).  
<sup>24</sup>K. I. Kugel and D. I. Khomskii, Sov. Phys. Usp. **25**, 231 (1982).  
<sup>25</sup>M. Matsuura, Y. Endoh, H. Hiraka, K. Yamada, K. Hirota, A. S. Mishchenko, N. Nagaosa, and I. V. Solovyev, J. Appl. Phys. **A74**, S792 (2002).